Published in final edited form as:
Dev Biol. 2007 April 15; 304(2): 556–566.

DIRECTED DIFFERENTIATION OF EMBRYONIC STEM CELLS INTO BLADDER TISSUE

Siam Oottamasathien[1,5,7], **YongQing Wang**[1], **Karin Williams**[1], **Omar E. Franco**[1], **Marcia L. Wills**[3], **John C. Thomas**[1,5], **Katrina Saba**[1], **Ali-Reza Sharif-Afshar**[1], **John H. Makari**[1,5], **Neil A Bhowmick**[1,2,4,5], **Romano T. DeMarco**[1,5], **Susan Hipkens**[6], **Mark Magnuson**[4,6], **John W. Brock III**[1,5], **Simon W. Hayward**[1,2,4], **John C. Pope IV**[1,5], and **Robert J. Matusik**[1,2,4]

1 *Department of Urologic Surgery, Vanderbilt University Medical Center, Nashville, Tennessee*

2 *Department of Cancer Biology, Vanderbilt University Medical Center, Nashville, Tennessee*

3 *Department of Pathology, Vanderbilt University Medical Center, Nashville, Tennessee*

4 *The Vanderbilt-Ingram Cancer Center, Vanderbilt University Medical Center, Nashville, Tennessee*

5 *Division of Pediatric Urology, Vanderbilt Children's Hospital Nashville, Tennessee*

6 *Center for Stem Cell Biology, Department of Physiology and Biophysics, Vanderbilt University Medical Center, Nashville, Tennessee*

Abstract

Manipulatable models of bladder development which interrogate specific pathways are badly needed. Such models will allow a systematic investigation of the multitude of pathologies which result from developmental defects of the urinary bladder. In the present communication, we describe a model in which mouse embryonic stem (ES) cells are directed to differentiate to form bladder tissue by specific interactions with fetal bladder mesenchyme. This model allows us to visualize the various stages in the differentiation of urothelium from ES cells, including the commitment to an endodermal cell lineage, with the temporal profile characterized by examining the induction of specific endodermal transcription factors (Foxa1 and Foxa2). In addition, final functional urothelial differentiation was characterized by examining uroplakin expression. It is well established that ES cells will spontaneously develop teratomas when grown within immunocompromised mouse hosts. We determined the specific mesenchymal to ES cell ratios necessary to dictate organ-specific differentiation while completely suppressing teratomatous growth. Embryonic mesenchyme is well established as an inductive tissue which dictates organ-specific programming of epithelial tissues. The present study demonstrates that embryonic bladder mesenchyme can also steer ES cells towards developing specific endodermal derived urothelium. These approaches allow us to capture specific stages of stem cell differentiation and to better define stem cell hierarchies.

INTRODUCTION

To elucidate the control of normal and abnormal bladder development, a model is needed that will allow the investigation from embryogenesis through adult differentiation. Multiple congenital disease states affect the bladder, including posterior urethral valves, bladder/cloacal

7) Author for correspondence at: Department of Urologic Surgery, A1302 MCN, Vanderbilt University Medical Center, Nashville, TN 37232-2765 Phone: 615-343-5604 Fax: 615-322-8990 e-mail: siam.oottamasathien@vanderbilt.edu

exstrophy, and myelomeningocele. In order to better understand these conditions, we developed a model using embryonic stem (ES) cells and tissue recombination. The model described follows the temporal-spatial events involved in bladder development and captures early protein expression patterns that have not previously been studied. These proteins may be unique to bladder stem and/or progenitor cells and could assist with their cellular isolation and characterization.

Instead of attempting to work from a mature bladder backwards to identify bladder stem and/or progenitor cells, we proposed starting from pluripotent ES cells which could be exposed to the strong inductive signaling properties of embryonic bladder mesenchyme (EBLM) to potentially direct formation of bladder tissues. Tissue recombination has led to a better understanding of bladder biology, especially with the premise that the mesenchyme is required to direct epithelial differentiation (Baskin et al., 1996a;Baskin et al., 1996b;DiSandro et al., 1998;Liu et al., 2000). We hypothesized that EBLM could dictate the differentiation of mouse ES cells into the endodermally derived bladder urothelial lineage. Undirected, grafted ES cells will form teratomas (Bradley et al., 1984;Gertow et al., 2004;Heins et al., 2004;Przyborski et al., 2004;Reubinoff et al., 2000;Thomson et al., 1998). This approach elucidates the process of bladder development and also offers the ability to identify bladder progenitor cells. Using ES cells in this approach, it is possible to generate other organs that require mesenchymal signals to differentiate (Taylor et al., 2006). Therefore, it should be possible to follow ES cell differentiation into germ-layer restricted progenitor cells that give rise to the fully mature organ. The characterization of these cell types is important with the potential applications for regenerative medicine and organ rehabilitation in disease states.

MATERIALS AND METHODS

Tissue Culture of Mouse Embryonic Stem Cells

Mouse ES cells (PluriStem B6-White; Chemicon International, Temecula, CA) were grown on a mitotically inactivated primary mouse embryonic fibroblast feeder layer in Iscove's modified Dulbecco's medium with 4mM L-glutamine and HEPES (IMDM; Hyclone, Logan, UT) supplemented with 20′ FCS (ES cell qualified, Hyclone), 0.1mM non-essential amino acids (Hyclone), 1mM sodium pyruvate (Hyclone), 0.1mM 2-mercaptoethanol (Sigma, St Louis, MO), 100U/ml penicillin (Sigma) and 100U/ml streptomycin (Sigma), and 1000U/ml leukemia inhibitory factor (ESGRO; Chemicon International). The medium was changed daily.

Tissue Recombination Grafts of Mouse Embryonic Stem Cells with Rat Embryonic Bladder Mesenchyme

All animal experiments were performed in accordance with the Institutional Animal Care and Use Committee at Vanderbilt University. Pregnant Sprague-Dawley rats (Harlan, Indianapolis, IN) were sacrificed at embryonic day 18 (plug day =0). The embryos were isolated and bladders removed. The bladders were separated from the urogenital sinus at the bladder neck prior to separation in Hanks/EDTA. The epithelial and mesenchymal components were microdissected, isolated, then washed thoroughly in RPMI-1640 (Gibco, Grand Island, NY) and stored in medium prior to use. ES cells were detached from their flasks by gentle trypsinization and viable cells counted on a hemocytometer using trypan blue exclusion. ES cells (50 – 1500 cells) were re-suspended in 40μl of rat collagen matrix and plated as a plug. This plug formed a half-oval like structure measuring 3 mm in widest diameter and 2 mm in height. EBLM, now left as pure mesenchymal shells devoid of epithelium (1 or 4 shells utilized per graft depending on the experimental condition) were physically placed into each collagen plug and then incubated at 37°C for plug solidification. Prior to grafting, each mesenchymal shell measured approximately 0.4 mm x 0.4 mm in size, therefore no difficulty was encountered when placing the shell(s) into the collagen plugs. Tissue culture media (RPMI-1640; [Gibco])

supplemented with 1′ antibiotic-antimycotic solution (Gibco), 5′ cosmic calf serum (CCS) (Hyclone) was then applied for one hour.

To obtain approximate cell numbers contained within individual EBLM shells, collagenase separation was performed. EBLM was reduced to single cells by a 90 min digestion at 37°C with 187 units/ml collagenase-lyophilized (Gibco, cat. # 17018-029) in RPMI-1640 tissue culture medium containing 10′ fetal bovine serum (Atlanta Biologicals, Lawrence, GA). Following digestion, the cells were washed extensively with RPMI-1640 tissue culture medium to remove traces of collagenase. Viable cells were then counted using a hemocytometer with trypan blue exclusion.

Athymic Nude Mouse Host Xenografting

Male athymic nude mice (CD-1 nu/nu Charles River) age 7–8 weeks were hosts for sub-renal capsule grafts. A 1 cm vertical skin incision along the dorsal midline was made and the kidney was introduced with gentle pressure. A capsulotomy was made in the kidney and a subcapsular space was created. Grafts were then placed underneath the renal capsule and maneuvered into various locations along the kidney. Two grafts were placed into each kidney which was then reintroduced back into the mouse. Surgical incisions were closed with suture and staples.

Xenograft Harvest and Processing

Hosts were sacrificed at 7, 14, and 42 days post grafting. Mice were sacrificed by anesthetic overdose followed by cervical dislocation. Grafts were harvested and the kidneys removed en-bloc. Whole kidneys were placed in 10′ neutral buffered formalin for 24 hours. After fixation, grafts were trimmed leaving a margin of renal parenchyma to aid in graft orientation. Specimens were processed, paraffin embedded, and sections cut at 5μm for staining and immunohistochemistry (IHC).

In addition, normal mouse tissues were examined and served as controls which included: embryonic day 16 (E16), postnatal day 1, and adult (6 months of age) mouse bladders. Tissues were processed and embedded in the same fashion as the xenografts, then cut in 5μm sections for staining and IHC.

Staining and Immunohistochemistry

Sections for Gomori’s trichrome staining were carried out with Gomori's OneStep Green Trichrome Stain System (DakoCytomation) and an automated stainer platform. This staining was performed by the Vanderbilt mouse histology core facility.

For IHC, all incubations were carried out at room temperature unless otherwise stated. Slides were deparaffinized and hydrated through xylene and graded alcohols. Antigen retrieval was performed on slides stained for Foxa1, Foxa2, p63, and Neun and achieved with microwaving in 1′ antigen unmasking solution (Vector laboratories, Burlingame, CA) for 20 min, then left at room temperature for 1 hour. Endogenous peroxidase activity was blocked with DAKO Peroxidase Blocking Reagent (DAKO Corp., Carpinteria, CA) for 15 min and sections were washed in PBS for 5 min. IHC was performed using the Vectastatin Elite ABC peroxidase kit (Vector Laboratories) according to the manufacturer’s protocol. Briefly, non-specific antibody binding was minimized by incubating sections for 20 min in diluted normal blocking serum. Sections were incubated overnight at 4°C in a humidified chamber with primary antibodies, at indicated dilutions were: broad-spectrum uroplakin (rabbit, 1:1000; a generous gift from Dr. TT Sun, New York University), smooth muscle α-actin (mouse, 1:1000; Sigma), p63 (rabbit, 1:200; Santa Cruz Biotechnology, Santa Cruz, CA), Foxa1 (goat, 1:1000; Santa Cruz), Foxa2 (goat, 1:1000; Santa Cruz), and neuronal nuclear antigen A60 (NeuN) (mouse, 1:100; Abcam, Cambridge, MA). Following overnight incubation, slides were washed in PBS for 5 min.

Sections were then incubated for 30 min with biotinylated secondary antibody solution diluted in PBS, followed by Vectastatin Elite ABC Reagent diluted in PBS for 30 min. Between incubations, sections were washed for 5 min in PBS. Visualization of immunoreactivity was achieved by incubating sections in either DAKO Liquid DAB Substrate-Chromogen System (DAKO Corp.) for 2–4 min or the DAB peroxidase substrate kit (Vector Laboratories) for 10 min. The sections were washed in double distilled H_2O, counterstained with hematoxylin, dehydrated, and cover slipped. Negative controls were set up at the same time as the primary antibody incubations and included incubation with PBS, in place of the primary antibody. No immunoreactivity was observed in these negative control sections.

Laser Capture Microdissection/DNA Isolation/Polymerase Chain Reaction

Tissue for laser capture microdissection (LCM) was collected prospectively following tissue processing and paraffin wax embedding. Approximately 1500 cells were microdissected from both urothelial compartments of the 42 day recombinant grafts using a Pix Cell II laser capture microscope (Arcturus, CA). As controls, tissue was also microdissected from native adult mouse and adult rat bladder tissue. DNA was extracted in lysis buffer containing 0.04′ proteinase K (New England BioLabs, Inc., Ipswich, MA), 10 mM Tris-HCL pH 8.0 (EM Science, Gibbstown, NJ), 1 mM EDTA (Sigma), 1′ Tween 20 (EM Science). Tissues were incubated in 50μl of lysis buffer overnight at 37°C, then boiled at 98°C for 8 minutes to degrade the proteinase K.

Total DNA was utilized for PCR utilizing mouse and rat species specific primers encoding for the probasin gene (mouse probasin gene product 302 bp, rat probasin gene product 420 bp). Mouse primers consisted of the following forward and reverse sequences: 5’-TCACATTTTGTGTGGGAGGA-3’ (forward) and 5’-CATATAATCACAACCCATCTCTTGA-3’ (reverse). Rat primers consisted of: 5’-TTGAAGGGAATTGGAGAACC-3’ (forward) and 5’-CATCCCTCCAGCCCTATCTA-3’ (reverse). PCR reactions were performed with Taq DNA polymerase (Sigma) in 25 μl reactions under the following scheme: 94°C for 5 minutes, then 30 cycles (94°C 45 seconds, 58°C 45 seconds, 68°C 90 seconds), then 68°C for 5 minutes. Final DNA products were detected on a 2′ agarose gel.

RESULTS

Bladder Development from Embryonic Stem Cells

Initial experiments were carried out with ES cells alone, without EBLM, to identify the number of ES cells necessary per graft to yield teratoma formation. Eight grafts (2 for each condition) were created by titrating numbers of ES cells as follows: 50, 100, 500, and 1000. Grafts were harvested at 42 days post in-vivo incubation. Grossly, grafts measured 3–10 mm in diameter, with smaller grafts (3–4 mm in diameter) observed at 50, 100, 500 ES cells and large tumors (7–10 mm in diameter) seen at 1000 cells (Fig. 1a). Consistent with an expectation of benign histology no gross invasion outside of the renal capsule or into the renal parenchyma was observed. H & E staining of the ES cell alone grafts at 50, 100, 500 cells revealed no significant growth or patterns of differentiation (data not shown). One thousand ES cells per graft yielded multiple well-differentiated structures forming teratomas, consistent with previous findings in the literature (Bradley et al., 1984;Gertow et al., 2004;Heins et al., 2004;Przyborski et al., 2004;Reubinoff et al., 2000;Thomson et al., 1998). Within the teratomas, tissue types from all 3 embryonic germ cell layers were present including cartilage, brain, skeletal muscle, neural structures, pancreatic, and intestinal tissue (Supplem. Fig. 8a–d). No evidence of spontaneous bladder tissue formation occurred in these ES cell derived teratomas, verified by negative uroplakin detection, a highly sensitive and specific marker for mature urothelium.

Next, 1 EBLM shell per graft (equivalent of 300,000 mesenchymal cells post collagenase separation) were recombined with titrating numbers of ES cells as follows: 50, 100, 500, and 1000 (n=8), then harvested after 42 days of incubation. Grossly, the tissue recombinants with the 50, 100, and 500 ES cell numbers measured 3–4 mm in diameter and had a paucity of growth with no evidence of bladder tissue formation. The 1000 ES cell recombinants were grossly larger in size measuring 7 – 10 mm in diameter and yielded multiple well differentiated structures forming as a teratoma, however a small population of tissues resembled bladder structures (Fig. 1b). These structures had central lumenoid cavities, a cluster of surrounding multi-layered epithelium, a sub-epithelial connective tissue layer consistent with lamina propria-like tissue, and smooth muscle fibrils. Immunolocalization of uroplakin verified mature bladder urothelial differentiation and was associated with the epithelial lining of the lumenoid structures (Fig. 1c). Figure 1d demonstrates smooth muscle α-actin (SMA) immunolocalization, indicating smooth muscle cell development, respectively surrounding mature urothelium. Overall, cellular organization and immunohistochemical staining was consistent with normal bladder tissue histology. These findings demonstrated that ES cells, under the inductive signaling environment provided by EBLM, could undergo complex differentiation along an endodermal lineage to form mature urothelium with bladder tissue formation.

Since 1000 ES cells + 1 EBLM shell per graft were sufficient to form a small population of bladder tissues within a teratoma, we created recombinants which consisted of 1500 ES cells + 4 EBLM shells per graft in attempt to further force the ES cells to form the bladder phenotype. Since we significantly increased the amount of EBLM per graft, the number of ES cells was increased to 1500 in order to optimize mesenchymal-ES cell interactions. A total of 4 recombinants were created and again harvested after 42 days of incubation. Grossly, the recombinants were smaller in size ranging from 2–3 mm in diameter. Gomori's trichrome staining of sections of all 4 recombinant grafts demonstrated 100′ bladder structures in each graft and all grafts exhibited no evidence of teratoma formation (Fig. 2a,b.; See Supplem. Fig. 9a–d for low power images). Only pure bladder tissue formation was observed, with absolutely no evidence for non-bladder structures adjacent to our ES cell derived bladder tissue. In addition, trichrome staining demonstrated a sub-epithelial connective tissue layer surrounding the urothelium, consistent with lamina propria-like tissue in combination with an outer smooth muscle layer as indicated by SMA immunolocalization (Fig. 2c,d). Uroplakin expression by the epithelia demonstrated mature urothelial differentiation and confirmed the bladder phenotype (Fig. 2e,f).

To better characterize the extent of bladder tissue development in the 1500 ES + 4 EBLM shells per graft recombinants, markers identifying endoderm were examined. The endodermal marker, Foxa1, was expressed in all of the recombinant urothelial cells (Fig. 3c). Organization of the recombinant urothelia was illustrated by using the basal cell marker, p63 (Fig. 3b). Immunohistochemical detection of p63 positive cells localized to the basilar urothelium only, with a marked lack of staining in the more central luminal urothelial cells.

As controls, grafts of 1 EBLM shell alone (n=10) and 4 EBLM shells alone (n=4) were performed and harvested after 42 days of incubation. H&E and Gomori's trichrome staining of the EBLM only grafts demonstrated a paucity of growth with no evidence of complex differentiation or bladder tissue formation (data not shown). These findings were consistent with data previously reported in the literature (Baskin et al., 1996a;Oottamasathien et al., 2006).

Identification of Bladder-Specific Stem and/or Progenitor Cells

In order to determine at what time period the ES cells begin to undergo an endodermal cell lineage transformation, experiments were performed to harvest recombinants at earlier

incubation periods. Recombinants of 1500 ES cells + 4 EBLM shells were grafted, then harvested at 7 and 14 day time points (n=6). Gomori's trichrome staining revealed the beginnings of cellular organization into bladder-like structures, yet the cells that looked destined to become urothelium still had significant disorder with mostly dysmorphic morphology (Fig. 4a,b). Uroplakin staining was performed on both the 7 and 14 day recombinant tissues but remained undetectable at this stage of development consistent with the lack of mature urothelium.

Spatial orientation, verified with p63 staining among the recombinant tissues, was undetectable in the 7 day tissues but began to occur in a small cohort of cells after 14 days of incubation (Fig. 4c,d). As previously identified, ES cells converted to urothelium had gained complete spatial orientation in the 42 day recombinant tissues, based on the basal expression of p63 (Fig. 3b). This illustrated a temporal relationship for p63 expression in basal cells of endodermal tissue, with the detection of endodermal markers preceding the ability to obtain orientation properties.

In the early developing prostate, Foxa2 is initially expressed in early embryonic developing glands, along with Foxa1. After birth, Foxa2 becomes undetectable and Foxa1 continues to be expressed in the mature ductal prostatic epithelium through adulthood (Gao et al., 2005). Since the prostate and bladder are both hindgut derivatives, the Fox family of proteins were chosen as endodermal target proteins of interest. In the recombinant time point grafts, both Foxa1 and Foxa2 were detected in the 7 day tissues (Fig. 4e,g). By day 14, both Fox proteins were abundant (Fig. 4f,h). As stated previously, Foxa1 was detected in all of the urothelial cells in the 42 day recombinants but interestingly, Foxa2 became almost extinguished in most cells and was intensely detectable in only a few cells (Fig. 3d).

In order to establish baseline protein expression patterns in normal mouse tissues, embryonic day 16 (E16), postnatal day 1, and adult mouse bladders were subjected to IHC staining for broad-spectrum uroplakin, p63, Foxa1, and Foxa2 (Fig's 5–7). Figure 5 shows that E16 mouse bladders fully express uroplakin, have p63 positive basal urothelium, Foxa1 expression in all urothelial cells, and scant Foxa2 expression. Figure's 6 and 7 illustrate that postnatal day 1 and adult mouse bladders share a similar profile, paralleling those observed in the E16 mouse bladders except Foxa2 was completely undetectable.

Laser Capture Microdissection/DNA Isolation/Polymerase Chain Reaction

To further verify that the recombinant urothelium within the 42 day grafts was of mouse origin, LCM was utilized to obtain tissue from various compartments. DNA samples were isolated from the recombinant urothelium, native adult mouse bladders (control), and native adult rat bladders (control). Polymerase chain reaction (PCR) was performed with mouse and rat specific primers for the probasin gene. Figure 10 (suppl.) illustrates the analysis of the mouse and rat probasin gene PCR products. This confirmed the mouse origin of the recombinant urothelium, yielding the 302 bp mouse probasin product. In summary, LCM coupled with DNA isolation and PCR was conclusive in defining the recombinant urothelial compartment as having originated from the mouse ES cells and not from potential rat urothelial contaminating elements in the EBLM preparation. As previously described, none of the EBLM alone grafts yielded bladder tissue growth, further substantiating that the EBLM preparations utilized were devoid of urothelial contaminants.

Development of Neuronal Tissue Associated with Bladder Recombinants

In the H&E stains of some sections, neuronal cell clusters formed having unique characteristics consistent with ganglionic tissue. Immunohistochemical detection for neuronal nuclear antigen A60 (NeuN) confirmed the neuronal nature of these cell clusters (Fig. 3e,f). NeuN staining

was also seen in individual cells interlaced within the smooth muscle layers. The NeuN antibody utilized was also tested on native mouse bladders (E16, postnatal day 1 and adult) and adult rat bladders. Positive staining was observed in only mouse tissue, with a complete lack of detection in the rat tissue, verifying species specificity of this antibody (data not shown). This illustrated that the neuronal cells present within the recombinants either originated from the ES cells or host mouse kidney, but they could not have arisen from the rat EBLM constituents.

DISCUSSION

In 1981, ES cells were isolated for the first time from mice. This major break through, revolutionized the field of developmental biology (Martin, 1981). ES cells can undergo prolonged self-renewal and differentiation, thus providing a tool to investigate the molecular mechanisms occurring during differentiation from the embryonic stage to the adult phenotype. These cells are considered to be pluripotent and can differentiate into almost all cells that arise from the three embryonic germ layers (Alison et al., 2002). In addition, ES cells can differentiate into multiple embryonic and adult cell type's in-vitro, but rarely cells of endodermal linage (Trounson, 2006). Differentiation in an in-vivo environment yields the full developmental potential of undifferentiated ES cell lines. For example, ES cells injected into severe combined immunodeficient (SCID) mice formed benign teratomas (Bradley et al., 1984;Gertow et al., 2004;Heins et al., 2004;Przyborski et al., 2004;Reubinoff et al., 2000;Thomson et al., 1998). In the ES cell teratomas, advanced differentiated structures from all three embryonic germ cell (EG) layers were present, including smooth muscle, bone, cartilage, gut, respiratory epithelium, keratinizing squamous epithelium, hair, neural epithelium, and ganglia.

The presence of stem and/or progenitor cells within the bladder is unknown, but hypothetically should exist. To identify stem cells within the vast population of cells in the bladder would be challenging, especially without bladder specific stem/progenitor cell markers. In attempt to identify bladder stem cells, we forced ES cells to differentiate into bladder structures rather than a teratoma. Thus, we document a transition of the ES cells to early endoderm and then to the progenitor cells that give rise to bladder stem cells and thence urothelium. Rather than isolating a stem cell, we were watching it develop.

We hypothesized that if we can harness ES cells to produce other organs rather than teratomas, we will have a unique opportunity to investigate the molecular pathways that determine the stem cells for multiple organs during embryonic development. In order to study these pathways, it is important to achieve almost 100′ conversion of the ES cell to only one tissue type. Recently Taylor et al. (Taylor et al., 2006) reported that human embryonic stem cells recombined with rat urogenital mesenchyme (UGM) gave rise to immature and mature human prostate tissue, supporting the hypothesis that specific organ tissues can be influenced by inductive mesenchyme to form from ES cells. Although, the precise inductive events regulating embryonic pattern formation are still unknown; it is known that UGM isolated from embryonic day 18 urogenital sinus can induce freshly isolated adult bladder urothelium to develop a prostate (Aboseif et al., 1999;Donjacour and Cunha, 1993;Neubauer et al., 1983) and that the UGM is required for prostate development (Cunha, 1972). Although this inductive nature of UGM is well established, it is unknown whether the bladder urothelium undergoes a trans-differentiation to prostatic epithelium or if bladder and prostate share a common stem cell that is controlled by different inductive mesenchyme.

Initial experiments showed that no significant growth and differentiation into teratomas occurred at less than 500 ES cells per graft. At 1000 cells per graft, complex structures representing a teratoma occurred. Staining for a urothelial marker, uroplakin, confirmed the

lack of bladder tissues spontaneously developing. Although theoretically ES cells could generate urothelium and bladder tissues within a teratoma, it was important to determine the minimum number of ES cells needed to form a teratoma with the goal of redirecting these ES cells to form only one organ type.

Based upon the findings that 1000 ES cells + 1 EBLM shell per graft yielded small foci of uroplakin expressing bladder tissue within a teratoma, we hypothesized that the system could be pushed further to form only pure bladder tissue devoid of teratomatous elements by simply increasing the ratio of EBLM to ES cells. We empirically increased both the number of EBLM shells from one to four in each graft, along with optimizing the number of ES cells from 1000 to 1500. This ratio proved to be successful, the recombinants no longer exhibited teratoma structures, only pure uroplakin expressing urothelium with mature bladder tissues. Amazingly, the ES cells conversion into mature urothelium exhibited cellular organization that was complex such that the basilar located cells were p63 positive and the central luminal urothelium remained p63 negative. Within the recombinant stromal compartment, smooth muscle layers correctly differentiated and neuronal cells organized to form ganglionic tissue. Additional neuronal cells were also present interlaced among smooth muscle fibrils. These neuronal elements most likely originated from the ES cells but we cannot rule out the host kidney as the source. Clearly, the neuronal cells did not develop from the rat EBLM since we confirmed the mouse species specificity of these cells with the NeuN antibody. No other reports have shown that neuronal elements would develop in bladder tissue following a recombination of bladder urothelium with bladder mesenchyme. Remarkably, the conversion of ES cells to the bladder phenotype exhibited all the cellular organization required for a functional bladder.

Embryonic bladders can only be readily identified around 14 days of gestation in the mouse. Therefore the earlier events that orchestrate endodermal lineage differentiation have been impossible to investigate. Each stage that occurs in the recombinant tissues reflects stages of ES cells conversion into endoderm, then from endoderm to bladder stem cells, then from stem cells to mature urothelium within bladder tissue. Further studies will be needed to follow their complete developmental progression.

No studies or models to date have described endodermal lineage protein expression patterns in the developing bladder to adult maturation. In our time point experiments, we first detected the endodermal markers of Foxa1 and Foxa2 at 7 days, then extensively by 14 days. During these stages, uroplakin was undetectable, consistent with studies that have shown that immature urothelium does not express uroplakin (Lavelle et al., 2002;Romih et al., 1998). Although these cells were endodermal and looked destined to become urothelium, they were not mature urothelium at these two early time points.

Since little is known about the gene expression patterns in the developing bladder, we based our experimental parameters on what is known in the prostate since both organs are hindgut derivatives. Mirosevich et al. (Mirosevich et al., 2005) reported that embryonic day 18 rodent prostate and bladders express Foxa1 in the epithelial compartments and Besnard et al. (Besnard et al., 2004) identified Foxa1 expression in the urothelium of adult bladders. It is known that Foxa2 expression in the developing prostate occurs in very early epithelial budding during embryogenesis and that its expression coincides with Foxa1 expression (Mirosevich et al., 2005). As the developing prostate forms more mature glands, Foxa1 expression is retained in the epithelium through adulthood and Foxa2 is extinguished post-natally. Our findings parallel those in the prostate, Foxa1 and Foxa2 expression were detected early in the 7 and 14 day recombinants, but by 42 days only Foxa1 remained and Foxa2 was almost undetectable. We also performed IHC with antibodies to both Fox proteins in native E16, postnatal day 1, and adult mouse bladders. In E16 tissues, Foxa1 was expressed in all urothelium with Foxa2 expression limited to only a few cells. In postnatal day 1 and adult bladder tissues, Foxa1 was

again expressed in all urothelium but Foxa2 expression was completely undetectable. These findings illustrate a temporal relationship of Foxa protein expression patterns that have not been previously reported in the bladder and it demonstrates the potential power to use this model not only in studying bladder development but in other organ systems as well. These findings capture a time period during development illustrating that Foxa2 is highly expressed early in bladder progenitor cells, then completely turns off in mature urothelium. The exact role of the Fox proteins in bladder development remains unclear, although we have demonstrated a novel model in which to characterize endodermal related events involved in bladder embryogenesis.

Overall, developmental models are lacking in which to study embryonic differentiation into a specific organ. We have shown that mouse ES cells, in the appropriate inductive signaling environment, can undergo endodermal lineage transformation into mature urothelium. Our model yields a powerful example of the temporal and spatial events occurring during endodermal differentiation of the bladder. These findings suggest that ES cells can be controlled to differentiate into specific organs opening up the opportunity to characterize the molecular and cellular events that give rise to organ stem cells.

Supplementary Material

Refer to Web version on PubMed Central for supplementary material.

Acknowledgements

This research was supported by National Institutes of Health Grant to John C. Pope IV (R01-DK068593) and the Frances Williams Preston Laboratories of the T.J. Martell Foundation to Robert J. Matusik.

References

Aboseif S, El-Sakka A, Young P, Cunha G. Mesenchymal reprogramming of adult human epithelial differentiation. Differentiation 1999;65:113–8. [PubMed: 10550544]

Alison MR, Poulsom R, Forbes S, Wright NA. An introduction to stem cells. J Pathol 2002;197:419–23. [PubMed: 12115858]

Baskin LS, Hayward SW, Young P, Cunha GR. Role of mesenchymal-epithelial interactions in normal bladder development. J Urol 1996a;156:1820–7. [PubMed: 8863624]

Baskin LS, Hayward SW, Young PF, Cunha GR. Ontogeny of the rat bladder: smooth muscle and epithelial differentiation. Acta Anat (Basel) 1996b;155:163–71. [PubMed: 8870784]

Besnard V, Wert SE, Hull WM, Whitsett JA. Immunohistochemical localization of Foxa1 and Foxa2 in mouse embryos and adult tissues. Gene Expr Patterns 2004;5:193–208. [PubMed: 15567715]

Bradley A, Evans M, Kaufman MH, Robertson E. Formation of germ-line chimaeras from embryo-derived teratocarcinoma cell lines. Nature 1984;309:255–6. [PubMed: 6717601]

Cunha GR. Tissue interactions between epithelium and mesenchyme of urogenital and integumental origin. Anat Rec 1972;172:529–41. [PubMed: 5011946]

DiSandro MJ, Li Y, Baskin LS, Hayward S, Cunha G. Mesenchymal-epithelial interactions in bladder smooth muscle development: epithelial specificity. J Urol 1998;160:1040–6. [PubMed: 9719273] discussion 1079

Donjacour AA, Cunha GR. Assessment of prostatic protein secretion in tissue recombinants made of urogenital sinus mesenchyme and urothelium from normal or androgen-insensitive mice. Endocrinology 1993;132:2342–50. [PubMed: 7684975]

Gao N, Ishii K, Mirosevich J, Kuwajima S, Oppenheimer SR, Roberts RL, Jiang M, Yu X, Shappell SB, Caprioli RM, Stoffel M, Hayward SW, Matusik RJ. Forkhead box A1 regulates prostate ductal morphogenesis and promotes epithelial cell maturation. Development 2005;132:3431–43. [PubMed: 15987773]

Gertow K, Wolbank S, Rozell B, Sugars R, Andang M, Parish CL, Imreh MP, Wendel M, Ahrlund-Richter L. Organized development from human embryonic stem cells after injection into immunodeficient mice. Stem Cells Dev 2004;13:421–35. [PubMed: 15345136]

Heins N, Englund MC, Sjoblom C, Dahl U, Tonning A, Bergh C, Lindahl A, Hanson C, Semb H. Derivation, characterization, and differentiation of human embryonic stem cells. Stem Cells 2004;22:367–76. [PubMed: 15153613]

Lavelle J, Meyers S, Ramage R, Bastacky S, Doty D, Apodaca G, Zeidel ML. Bladder permeability barrier: recovery from selective injury of surface epithelial cells. Am J Physiol Renal Physiol 2002;283:F242–53. [PubMed: 12110507]

Liu W, Li Y, Cunha S, Hayward G, Baskin L. Diffusable growth factors induce bladder smooth muscle differentiation. In Vitro Cell Dev Biol Anim 2000;36:476–84. [PubMed: 11039497]

Martin GR. Isolation of a pluripotent cell line from early mouse embryos cultured in medium conditioned by teratocarcinoma stem cells. Proc Natl Acad Sci U S A 1981;78:7634–8. [PubMed: 6950406]

Mirosevich J, Gao N, Matusik RJ. Expression of Foxa transcription factors in the developing and adult murine prostate. Prostate 2005;62:339–52. [PubMed: 15389796]

Neubauer BL, Chung LW, McCormick KA, Taguchi O, Thompson TC, Cunha GR. Epithelial-mesenchymal interactions in prostatic development. II. Biochemical observations of prostatic induction by urogenital sinus mesenchyme in epithelium of the adult rodent urinary bladder. J Cell Biol 1983;96:1671–6. [PubMed: 6853598]

Oottamasathien S, Williams K, Franco OE, Thomas JC, Saba K, Bhowmick NA, Staack A, Demarco RT, Brock JW 3rd, Hayward SW, Pope JCt. Bladder tissue formation from cultured bladder urothelium. Dev Dyn 2006;235:2795–801. [PubMed: 16804891]

Przyborski SA, Christie VB, Hayman MW, Stewart R, Horrocks GM. Human embryonal carcinoma stem cells: models of embryonic development in humans. Stem Cells Dev 2004;13:400–8. [PubMed: 15345134]

Reubinoff BE, Pera MF, Fong CY, Trounson A, Bongso A. Embryonic stem cell lines from human blastocysts: somatic differentiation in vitro. Nat Biotechnol 2000;18:399–404. [PubMed: 10748519]

Romih R, Jezernik K, Masera A. Uroplakins and cytokeratins in the regenerating rat urothelium after sodium saccharin treatment. Histochem Cell Biol 1998;109:263–9. [PubMed: 9541475]

Taylor RA, Cowin PA, Cunha GR, Pera M, Trounson AO, Pedersen J, Risbridger GP. Formation of human prostate tissue from embryonic stem cells. Nat Methods 2006;3:179–81. [PubMed: 16489334]

Thomson JA, Itskovitz-Eldor J, Shapiro SS, Waknitz MA, Swiergiel JJ, Marshall VS, Jones JM. Embryonic stem cell lines derived from human blastocysts. Science 1998;282:1145–7. [PubMed: 9804556]

Trounson A. The production and directed differentiation of human embryonic stem cells. Endocr Rev 2006;27:208–19. [PubMed: 16434509]

Abbreviations

(ES)
: embryonic stem cells

(EBLM)
: embryonic bladder mesenchyme

(SMA)
: smooth muscle α-actin

(E16)
: embryonic day 16

(LCM)
: laser capture microdissection

(NeuN)

neuronal nuclear antigen A60

(UGM)

urogenital mesenchyme

(PCR)

polymerase chain reaction

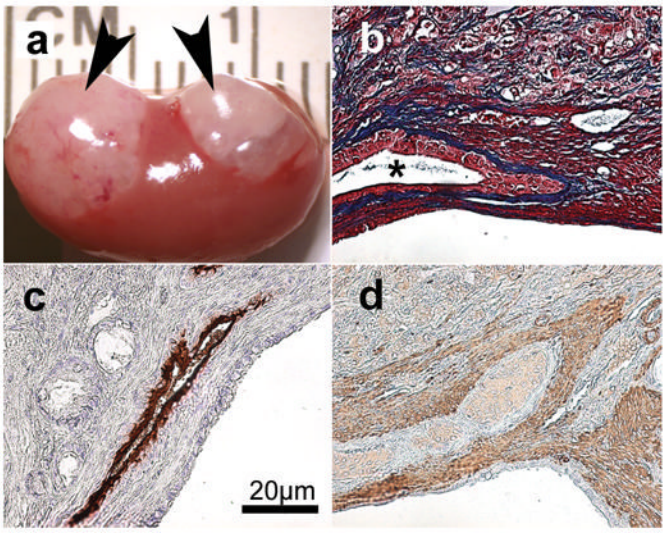

Figure 1.

Xenografts harvested at 42 days. *a.* Gross appearance of 1000 embryonic stem (ES) cell grafts on host kidney (arrowheads denote whitish-tan appearing grafts). *b–d.* Histology and immunohistochemical staining of 1000 ES cell + 1 embryonic bladder mesenchyme shell recombinant graft. *b.* Gomori's trichrome, star denotes central lumen of bladder structure, urothelial cells surrounding central lumen (red) with sub-urothelial connective tissue (blue) were seen. *c.* Immunohistochemical detection of broad-spectrum uroplakin (brown) denoting mature urothelium. *d.* Immunohistochemical detection of smooth muscle α-actin (brown) denoting smooth muscle fibrils.

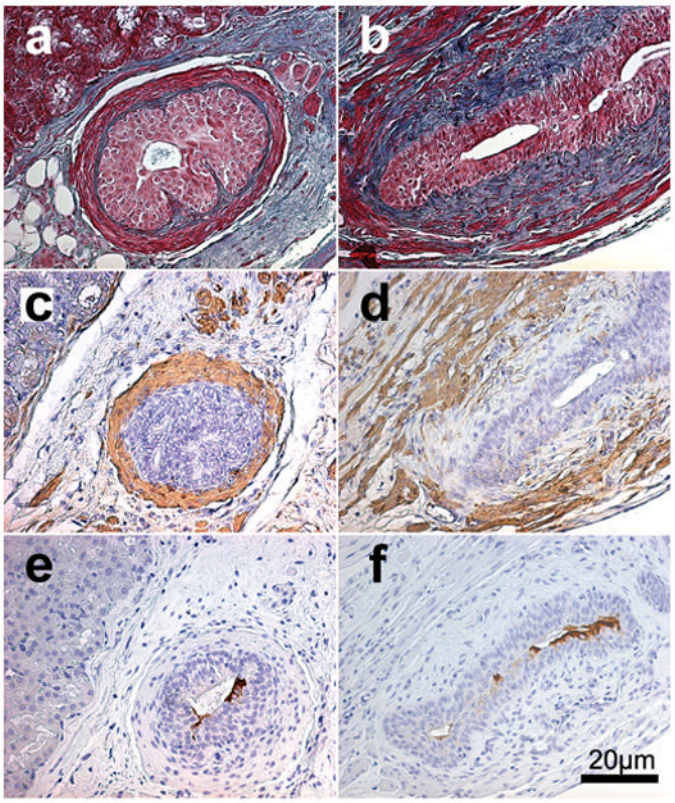

Figure 2.

Xenografts of 1500 embryonic stem cells + 4 embryonic bladder mesenchymal shells/graft harvested at 42 days. *a&b.* Gomori's trichrome, multilayered cuboidal urothelial cells (red) with sub-urothelial connective tissue (blue) were seen. *c&d.* Immunohistochemical detection of smooth muscle α-actin (brown) denoting smooth muscle fibrils. *e&f.* Immunohistochemical detection of broad-spectrum uroplakin (brown) denoting mature urothelium.

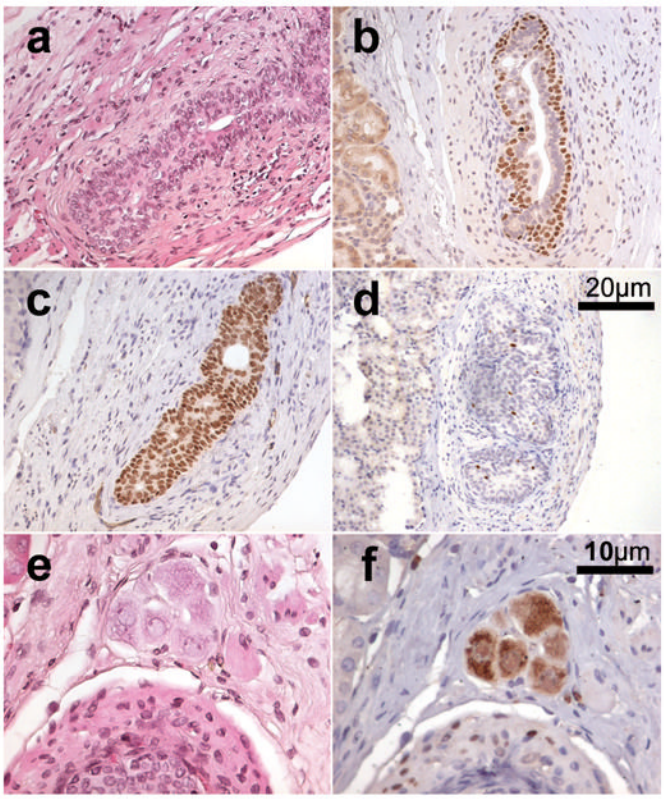

Figure 3.

Xenografts of 1500 embryonic stem (ES) cells + 4 embryonic bladder mesenchymal shells/graft harvested at 42 days. *a*. H&E staining. *b*. Immunohistochemical detection of p63 (brown) illustrating complete spatial orientation of ES cell derived urothelium. *c*. Immunohistochemical detection of Foxa1 (brown) seen in all ES cell derived urothelium. *d*. Immunohistochemical detection of Foxa2 (brown) seen strongly positive in only a few urothelial cells. *e&f*. H&E and immunohistochemical detection of neuronal nuclear antigen A60 (NeuN) (brown) confirming the presence of neuronal cells clustering in the form of a ganglion. Scale bars of 20 μm apply to images *a–d*. Scale bars of 10 μm apply to images *e&f*.

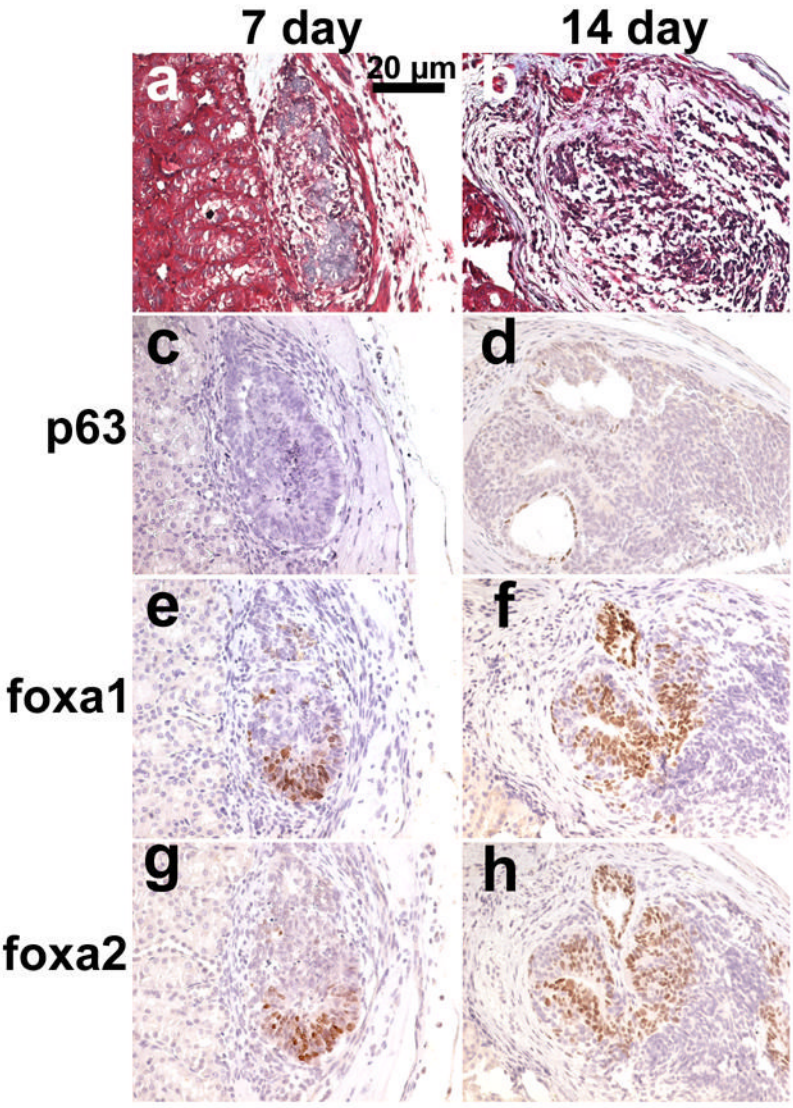

Figure 4.

Xenografts of 1500 embryonic stem cells + 4 embryonic bladder mesenchymal shells/graft harvested at 7 (*a,c,e,g*) and 14 (*b,d,f,h*) days. *a&b.* Gomori's trichrome, cellular organization occurring in cells that look destined to become urothelium (blue). *c&d.* Immunohistochemical detection of p63 (brown) illustrating lack of expression within 7 day tissues and early expression observed in 14 day tissues. *e&f.* Immunohistochemical detection of Foxa1 (brown) denoting endodermal cells. *g&h.* Immunohistochemical detection of Foxa2 (brown) denoting endodermal cells.

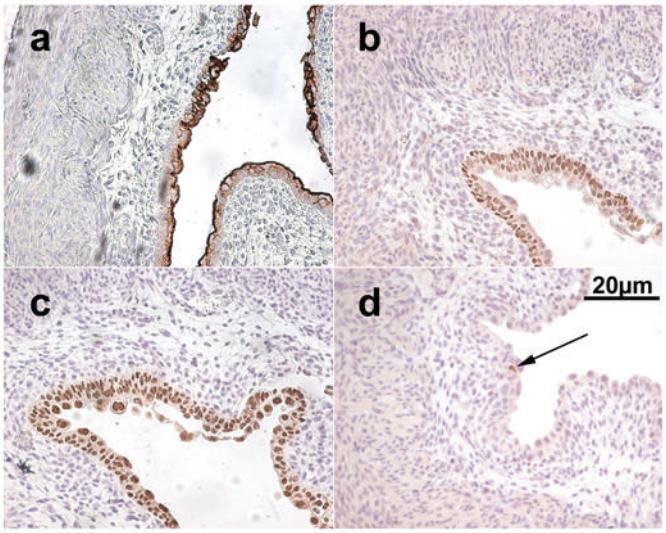

Figure 5.

Native embryonic day 16 mouse bladder. *a.* Immunohistochemical detection of broad-spectrum uroplakin (brown) denoting mature urothelium. *b.* Immunohistochemical detection of p63 (brown) demonstrating urothelial basilar orientation. *c.* Immunohistochemical detection of Foxa1 (brown) seen in all urothelial cells denoting endodermal derivation of the cells. *d.* Immunohistochemical detection of Foxa2 (brown), arrow denotes one positive staining cell within the section.

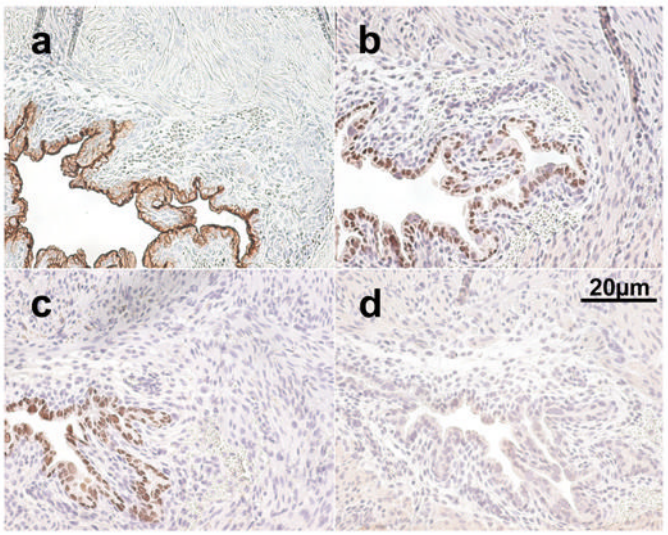

Figure 6.

Native postnatal day 1 of life mouse bladder. *a.* Immunohistochemical detection of broad-spectrum uroplakin (brown) denoting mature urothelium. *b.* Immunohistochemical detection of p63 (brown) demonstrating urothelial basilar orientation. *c.* Immunohistochemical detection of Foxa1 (brown) seen in all urothelial cells denoting endodermal derivation of the cells. *d.* Complete lack of immunohistochemical detection of Foxa2.

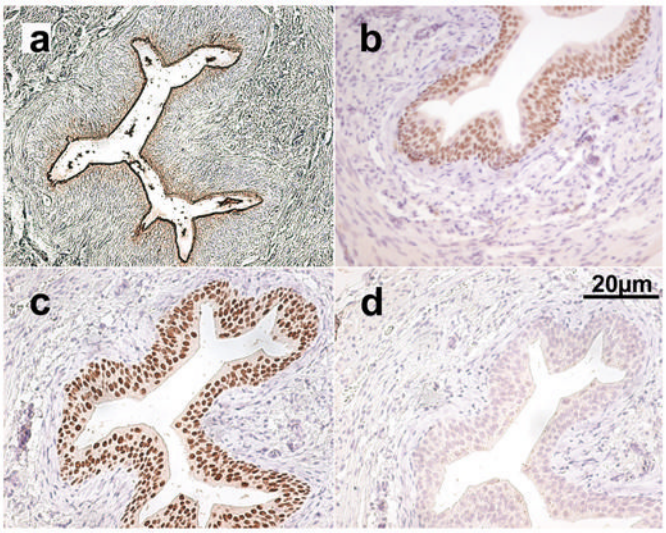

Figure 7.

Native adult mouse bladder. *a.* Immunohistochemical detection of broad-spectrum uroplakin (brown) denoting mature urothelium. *b.* Immunohistochemical detection of p63 (brown) demonstrating urothelial basilar orientation. *c.* Immunohistochemical detection of Foxa1 (brown) seen in all urothelial cells denoting endodermal derivation of the cells. *d.* Complete lack of immunohistochemical detection of Foxa2.